

Searching supersymmetry at the LHCb with displaced vertices

F. de Campos*

Departamento de Física e Química, Universidade Estadual Paulista, Guaratinguetá – SP, Brazil

O. J. P. Éboli†

Instituto de Física, Universidade de São Paulo, São Paulo – SP, Brazil.

M. B. Magro‡

Faculdade de Engenharia, Centro Universitário Fundação Santo André, Santo André – SP, Brazil.

D. Restrepo§

Instituto de Física, Universidad de Antioquia - Colombia

(Dated: October 22, 2018)

Supersymmetric theories with bilinear R–parity violation can give rise to the observed neutrino masses and mixings. One important feature of such models is that the lightest supersymmetric particle might have a sufficiently large lifetime to produce detached vertices. Working in the framework of supergravity models we analyze the potential of the LHCb experiment to search for supersymmetric models exhibiting bilinear R–parity violation. We show that the LHCb experiment can probe a large fraction of the $m_0 \otimes m_{1/2}$, being able to explore gluino masses up to 1.3 TeV. The LHCb discover potential for this kind of models is similar to the ATLAS and CMS ones in the low luminosity phase of operation of the LHC.

PACS numbers: 12.10.Dm, 12.60.Jv, 14.60.St, 98.80.Cq

*Electronic address: camposc@feg.unesp.br

†Electronic address: eboli@fma.if.usp.br

‡Electronic address: magro@fma.if.usp.br

§Electronic address: restrepo@uv.es

I. INTRODUCTION

Recently neutrino physics not only has firmly established a signal of physics beyond the Standard Model (SM) but also provided us valuable precise information on neutrino masses and mixings. Extensions of the Standard Model should address the neutrino mass generation mechanism, being able to accommodate the present neutrino knowledge. On the other hand, weak scale supersymmetry (SUSY) is a very popular solution for the hierarchy problem which also presents some pleasant features like the unification of the gauge couplings and the fact of being perturbative. R-parity conservation is an *ad-hoc* working hypothesis in SUSY models which can be violated. Moreover, it has been shown that SUSY models with R-parity non-conservation can generate neutrino masses and mixings, in particular, models with bilinear R-parity violation provide an economical effective model for supersymmetric neutrino masses [1, 2, 3, 4, 5, 6].

It is an experimental fact that supersymmetry is broken in the observed universe, however, little is known on how this break takes place. In this work we assume, for the sake of simplicity, gravity mediated supersymmetry breaking. Although R-parity violation can be introduced in a variety of ways [7, 8, 9, 10, 11] we work in the scenario of bilinear R-parity violation (BRpV). We call this model BRpV-mSUGRA. One nice feature of this model is that it is falsifiable at the CERN Large Hadron Collider despite the smallness of R-parity violation needed to accommodate the neutrino oscillation data [12, 13].

In BRpV-mSUGRA models the lightest supersymmetric particle (LSP) is no longer stable due to R-parity violating interactions. Moreover, the LSP can be rather long lived due to the smallness of the BRpV parameter needed to fit the neutrino masses and mixings [13, 14]. This opens a new window for SUSY studies, that is, the search for detached vertices associated to the decay of rather heavy particles. Although the LHCb experiment is not able to search for SUSY in the canonical signatures due to its non-hermicity, it does have good vertexing capabilities which allow for the SUSY searches in R-parity violating scenarios [13, 15]. Furthermore, the predicted BRpV-mSUGRA displaced vertices possess a visible invariant mass much larger than any SM particle, therefore, the search for displaced vertices is essentially background free.

In this work we study the potential of the LHCb experiment to search for BRpV-mSUGRA, showing that it can explore a large fraction of the $m_0 \otimes m_{1/2}$ plane. At small m_0 , the LHCb experiment will be able to study $m_{1/2}$ as high as 600 GeV which corresponds to neutralino masses of the order of 250 GeV and 1.3 TeV gluino masses. For $m_{1/2} = 500$ GeV the LHCb has a large m_0 reach which extends to $\simeq 2$ TeV. It is interesting to notice that the LHCb reach is just $\approx 30\%$ smaller than the ATLAS and CMS ones in the initial operation of the LHC, that is, in the low luminosity phase.

Previously, the search for SUSY via displaced vertices at the LHCb has been studied in Ref. [15], however, this work considered explicit R-parity breaking via baryon number violating operators (λ''), which leads to pure hadronic neutralino decays $\tilde{\chi}_1^0 \rightarrow qq\bar{q}$. Our BRpV-mSUGRA model differs from that scenario in many ways since the R-parity violating parameters are rather constrained by neutrino physics, which, in turn, restrict the branching ratios and decay lengths of the LSP. Moreover, the lightest neutralino does not possess pure hadronically decay modes, decaying into pure leptonic channels or in semileptonic modes; see Section II for further details. Since the LHCb experiment has already designed a dimuon trigger, it should be straightforward to look for $\tilde{\chi}_1^0 \rightarrow \nu\mu^+\mu^-$ events originated from our BRpV-mSUGRA model.

This paper is organized as follows. In Sect. II we present the BRpV-mSUGRA model and its main properties. The details of our analysis, our results and conclusions are in Sect. III.

II. MODEL PROPERTIES

The superpotential for the supergravity model with bilinear R-parity violation is [1]

$$W_{\text{BRpV}} = W_{\text{MSSM}} + \varepsilon_{ab} \epsilon_i \widehat{L}_i^a \widehat{H}_u^b, \quad (1)$$

where W_{MSSM} is the usual potential of the minimal supersymmetric standard model and the additional bilinear contribution contains three parameters (ϵ_i), one for each fermion generation. The BRpV–mSUGRA model also possesses new soft supersymmetry breaking terms

$$V_{\text{soft}} = V_{\text{mSUGRA}} - \varepsilon_{ab} B_i \epsilon_i \widetilde{L}_i^a H_u^b \quad (2)$$

with three new free parameters (B_i). It is interesting to notice that there is no field redefinition such that the BRpV terms of the superpotential and the associated soft terms can be eliminated simultaneously. Moreover, the bilinear R–parity violating interactions generate a vacuum expectation value for the sneutrino fields (v_i) after the minimization of the full scalar potential.

In total, the BRpV–mSUGRA model has eleven free parameters which are

$$m_0, m_{1/2}, \tan \beta, \text{sign}(\mu), A_0, \epsilon_i, \text{ and } B_i, \quad (3)$$

where $m_{1/2}$ and m_0 are the common gaugino mass and scalar soft SUSY breaking masses at the unification scale, A_0 is the common trilinear term, and $\tan \beta$ is the ratio between the Higgs field vacuum expectation values.

In the BRpV–mSUGRA model neutralinos and neutrinos mix via the BRpV interactions and through the induced sneutrino vacuum expectation values, giving rise to a 7×7 neutral fermion mass matrix. At tree level these models exhibit just one massive neutrino at the atmospheric scale while solar mass scale comes into play via one–loop radiative corrections [3, 4, 12, 16]. It has been shown in Refs. [3, 4] that the neutrino masses and mixings stemming from the diagonalization of the neutral fermion mass matrix are approximately given by

$$\begin{aligned} \Delta m_{12}^2 &\propto |\vec{\epsilon}| & ; & \quad \Delta m_{23}^2 \propto |\vec{\Lambda}| \\ \tan^2 \theta_{12} &\sim \frac{\epsilon_1^2}{\epsilon_2^2} & ; & \quad \tan^2 \theta_{13} \approx \frac{\Lambda_2^2}{\Lambda_2^2 + \Lambda_3^2} \\ \tan^2 \theta_{23} &\approx \frac{\Lambda_2^2}{\Lambda_3^2} \end{aligned} \quad (4)$$

where we defined $\Lambda_i = \epsilon_i v_d + \mu v_i$ and we denoted $|\vec{\Lambda}| = \sqrt{\Lambda_1^2 + \Lambda_2^2 + \Lambda_3^2}$ and similarly for $|\vec{\epsilon}|$.

It is convenient to trade the soft parameters B_i by Λ_i since these are more directly related to the neutrino–neutralino mass matrix. With this choice a point in the BRpV–mSUGRA parameter space is specified by

$$m_0, m_{1/2}, \tan \beta, \text{sign}(\mu), A_0, \epsilon_i, \text{ and } \Lambda_i. \quad (5)$$

Given a mSUGRA point, that is $m_0, m_{1/2}, \tan \beta, \text{sign}(\mu)$ and A_0 , the BRpV parameters ϵ_i and Λ_i are strongly constrained by the available neutrino physics data [17]. Therefore, the neutralino decay properties are rather well determined, usually varying by up to $\simeq 50\%$ when we consider solutions for ϵ_i and Λ_i compatible with the experimental neutrino mixings and squared mass differences at 3σ level,

that we considered to be [18],

$$\begin{aligned} \Delta m_{21}^2 &= 7.6_{-0.5}^{+0.7} \times 10^{-5} \text{ eV}^2 & ; & \quad \Delta m_{31}^2 = 2.4 \pm 0.4 \times 10^{-3} \text{ eV}^2, \\ \tan^2 \theta_{12} &= 0.47_{-0.12}^{+0.20} & ; & \quad \tan^2 \theta_{23} = 1.00_{-0.48}^{+1}, \\ \tan^2 \theta_{13} &< 0.05 \end{aligned} \tag{6}$$

In order to determine the BRpV parameters compatible with the neutrino data, we use an iterative procedure whose starting point is the approximated analytic results given in Eq. (4). In each iteration of the search procedure, the neutrino masses and mixing are obtained numerically and compared with their 3σ ranges given by Eq. (6). If Δm_{23}^2 is less (greater) than the experimental range, then the value of $|\vec{\Lambda}|$ is increased (decreased). The same is done for Δm_{12}^2 with $|\vec{\epsilon}|$. Once proper values for $|\vec{\Lambda}|$ and $|\vec{\epsilon}|$ are obtained, the interactions continues by changing the values for Λ_i and ϵ_i until a solution for the squared mass differences and mixing angles is obtained. Due to small neutrino masses, the BRpV interactions compatible with the neutrino data are rather weak, with $|\vec{\epsilon}|$ ($|\vec{\Lambda}|$) being of the order of 10^{-2} – 10^{-1} GeV (GeV^2).

In parameter space regions where the lightest neutralino is the LSP the BRpV interactions render the lightest neutralino unstable and can mediate two- and three-body LSP decays depending on the SUSY spectrum. Considering the new BRpV interactions the lightest neutralino can exhibit fully leptonic decays

$$\begin{aligned} \star \tilde{\chi}_1^0 &\rightarrow \nu \ell^+ \ell^- \text{ with } \ell = e \text{ or } \mu; \\ \star \tilde{\chi}_1^0 &\rightarrow \nu \tau^+ \tau^-; \\ \star \tilde{\chi}_1^0 &\rightarrow \nu \tau^\pm \ell^\mp; \end{aligned}$$

as well as semi-leptonic decay modes

$$\begin{aligned} \star \tilde{\chi}_1^0 &\rightarrow \nu q \bar{q}; \\ \star \tilde{\chi}_1^0 &\rightarrow \tau q' \bar{q}; \\ \star \tilde{\chi}_1^0 &\rightarrow \ell q' \bar{q}; \\ \star \tilde{\chi}_1^0 &\rightarrow \nu b \bar{b}. \end{aligned}$$

Notice, if kinematically allowed, some of these modes are generated in two steps. Initially we have a neutralino two-body decay, like $\tilde{\chi}_1^0 \rightarrow W^\mp \mu^\pm$, $\tilde{\chi}_1^0 \rightarrow W^\mp \tau^\pm$, $\tilde{\chi}_1^0 \rightarrow Z \nu$, or $\tilde{\chi}_1^0 \rightarrow h \nu$, followed by the Z , W^\pm or h decay; for further details see Ref. [13]. In addition to these channels there is also the possibility of the neutralino decaying invisibly into three neutrinos, however, this channel does not dominate in most of the parameter space.

We depicted in Figures 1 and 2 the main lightest neutralino branching ratios a function of $m_0 \otimes m_{1/2}$ for $A_0 = -100$ GeV, $\tan \beta = 10$, and $\mu > 0$. In the white region in the top left corner of this figure the lightest neutralino is no longer the LSP, that turns out to be the lightest charged scalar (S_1^\pm). In this region the $\tilde{\chi}_1^0$ decays promptly into $S_1^\pm \tau^\mp$. Moreover, the S_1^\pm decays so rapidly through BRpV interactions that it does not yield a displaced vertex. In the small m_0 where the lightest neutralino is the LSP and this decay is kinematically forbidden, the almost on-shell S_0^1 contribution dominates and the main LSP decay modes are $\nu \tau^+ \tau^-$ and $\nu \tau^\pm \ell^\mp$; see the lower panels of Fig. 1.

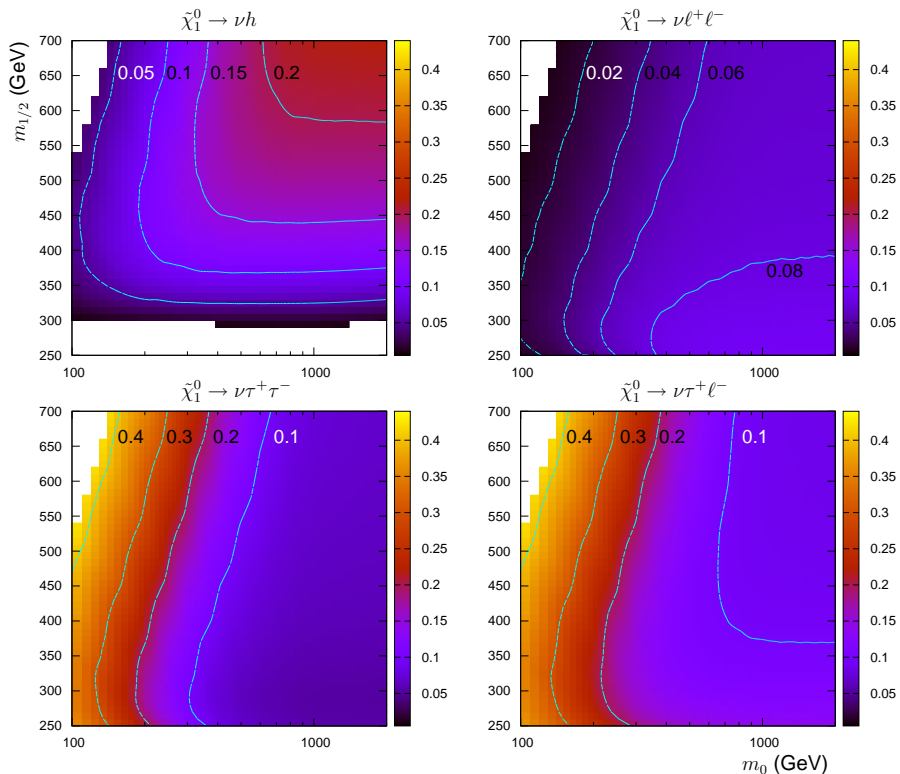


FIG. 1: Lightest neutralino branching ratios as a function of m_0 and $m_{1/2}$ for $A_0 = -100$ GeV, $\tan\beta = 10$, and $\mu > 0$. The upper left (right) panel presents the branching ratio into νh ($\nu \ell^+ \ell^-$) while the lower left (right) panel is for $\nu \tau^+ \tau^-$ ($\nu \ell^\pm \tau^\mp$).

We can see from the top right panel of Fig 1 that $\tilde{\chi}_1^0$ does have a sizeable branching ratio into νh , specially for heavier LSP and larger m_0 . Notice that this decay is kinematically forbidden in the white region in the bottom of this panel. From the other panels of this figure we can learn that the leptonic decay $\nu \ell^+ \ell^-$ with $\ell^\pm = \mu^\pm$ is of the order of a few to 10%, while the decay modes e^\pm , $\nu \tau^+ \tau^-$ and $\nu \tau^\pm \ell^\mp$ vary from $\approx 40\%$ at small m_0 to a few percent at large m_0 . At moderate and large m_0 , these decays originate from the lightest neutralino decaying into the two-body modes $\tau^\pm W^\mp$, $\mu^\pm W^\mp$ and νZ , followed by the leptonic decay of the weak gauge bosons.

In general, semi-leptonic decays of the LSP are suppressed at small m_0 and they dominate at large m_0 due to two-body decays; see Fig. 2. In fact, a closer look into this figure reveals that the dominant decay modes in this m_0 region are $\tau^\mp W^\pm \rightarrow \tau^\mp q' \bar{q}$, $\ell^\mp W^\pm \rightarrow \ell^\mp q' \bar{q}$, $\nu Z \rightarrow \nu q \bar{q}$, and $\nu h \rightarrow \nu b \bar{b}$. For a given value of $m_{1/2}$, the branching ratios into $\tau^\mp W^\pm$, νZ and $\ell^\mp W^\pm$ are dominant and rather similar. Moreover, the importance of the νh channel grows as $m_{1/2}$ increases in the moderate and large m_0 regions; these facts are illustrated in the right panel of Fig. 4 for a fixed value of $m_{1/2}$.

The BRpV–mSUGRA parameters needed to reproduce the present neutrino data are rather small [3, 4]. Therefore, the BRpV interactions responsible for the LSP decay are feeble, rendering the LSP long lived as can be seen from Figure 3. The left panel of this figure was obtained for $\tan\beta = 10$ and it shows that the $\tilde{\chi}_1^0$ decay length can be as large as a few millimeters for light neutralino masses. As the $\tilde{\chi}_1^0$

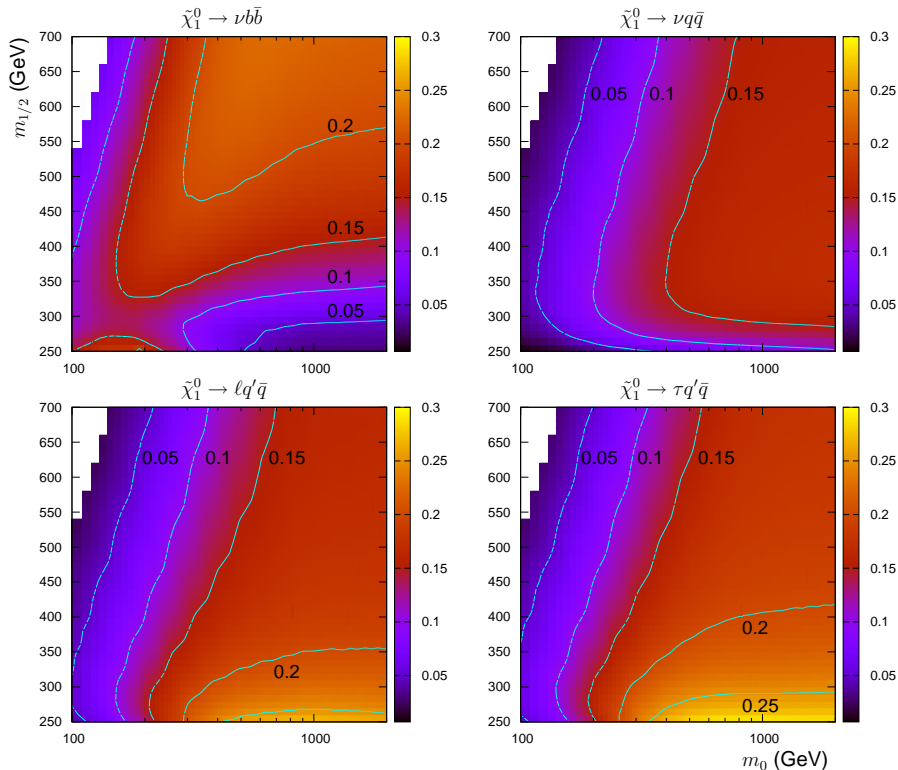


FIG. 2: Same as Figure 1 for the decays $\nu b \bar{b}$ (upper left panel), $\nu q \bar{q}$ (upper right panel), $\ell q' \bar{q}$ (lower left panel), and $\tau q' \bar{q}$ (lower right panel).

mass ($m_{1/2}$) increases its decay length shortens, however, it is still sizeable even for heavier neutralinos ($\simeq 100 \mu\text{m}$). Notice that for fixed values of $m_{1/2}$ the decay length is rather independent of m_0 . Another salient feature of the BRpV–mSUGRA model is that the neutralino decay length is rather insensitive to variations of the BRpV parameters provided they lead to neutrino masses and mixings compatible within 3σ with the allowed experimental results. We present in the left panel of Fig. 3 the effect of such variations of the BRpV parameters as bands for a fixed value of $m_{1/2}$.

In order to assess the dependence of our results on $\tan\beta$ we present in the right panel of Fig. 3 the lightest neutralino decay length as a function of m_0 for $\tan\beta = 40$. As we can see, the $\tan\beta = 40$ results are rather similar to the ones for $\tan\beta = 10$, except for the appearance of narrow regions where the $\tilde{\chi}_1^0$ decay length is drastically reduced. In these special regions the mixing between scalars (higgses and sfermions) is rather large which enhances some two–body decay channels. This can be seen more clearly by comparing the two panels of Fig. 4 where we present the LSP branching ratios as a function of m_0 for $\tan\beta = 10$ (left panel) and $\tan\beta = 40$ (right panel). The $\nu b \bar{b}$ (νh) has a sudden increase around $m_0 \simeq 750$ and 950 GeV due to the large sneutrino–neutral higgs mixing, while a large stau–charged Higgs mixing leads to a large increase of the $\nu \tau^\pm \tau^\mp$ mode around $m_0 \simeq 900$ GeV. In general these mixings are small since they are proportional to the square of the BRpV parameters divided by the difference of the squared MSSM masses [5], however, the mixings become quite large in the regions presenting almost degenerate states. Therefore, we can infer from Figure 4 that the general trend observed for $\tan\beta = 10$

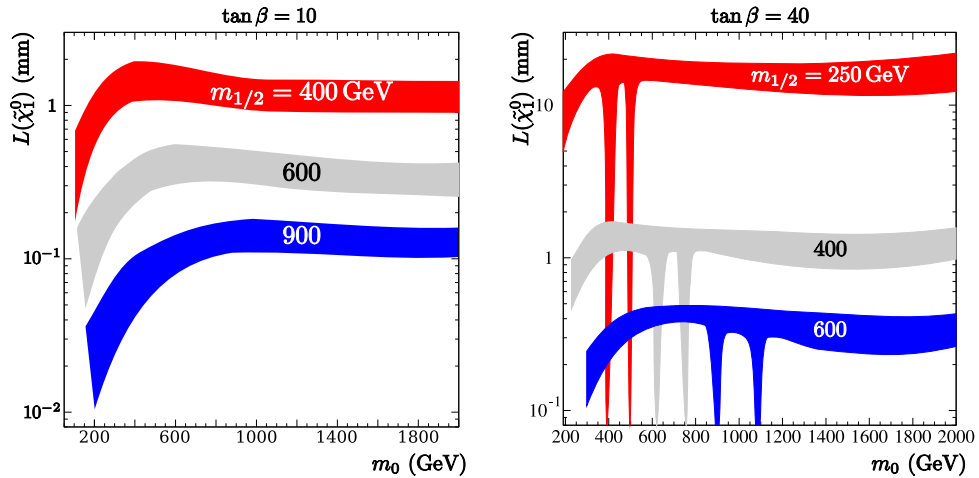


FIG. 3: $\tilde{\chi}_1^0$ decay length versus m_0 for $A_0 = -100$ GeV, $\mu > 0$, several values of $m_{1/2}$, and $\tan \beta = 10$ (left panel) and $\tan \beta = 40$ (right panel). The widths of the three shaded (colored) bands for fixed $m_{1/2}$ GeV correspond to the variation of the BRpV parameters in such a way that the neutrino masses and mixing angles fit the required values within 3σ [18].

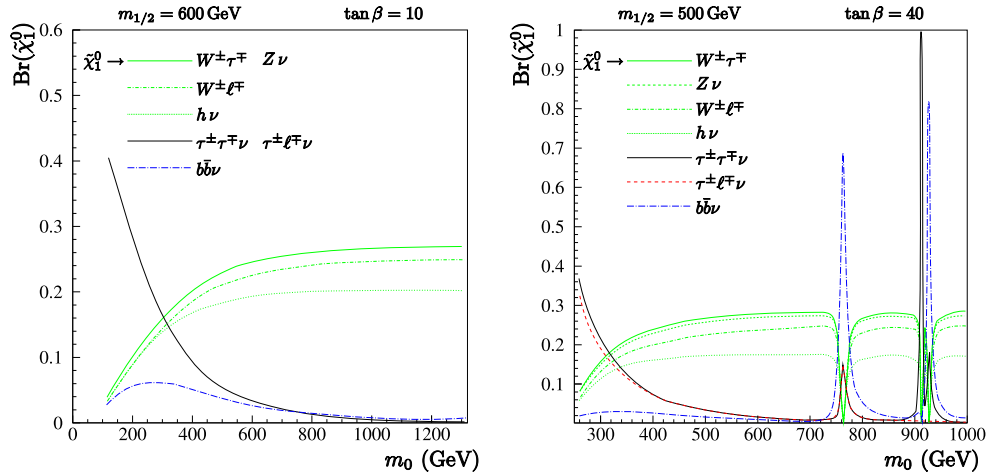


FIG. 4: $\tilde{\chi}_1^0$ branching ratios versus m_0 for $A_0 = -100$ GeV, $\mu > 0$, $m_{1/2} = 500$ GeV, and $\tan \beta = 10$ (left panel) or $\tan \beta = 40$ (right panel).

is maintained for $\tan \beta = 40$, except for the parameter space regions where sfermions and higgses are nearly degenerate.

The existence of long decay lengths is an important feature of the BRpV models since detached vertices are a smoking gun of SUSY with R-parity violation. Furthermore, displaced vertices provide an additional handle that makes possible the SUSY search at the LHCb experiment.

III. RESULTS AND CONCLUSIONS

Our goal is to assess the potential of the LHCb experiment to search for displaced vertices associated to the visible LSP decays. In order to generate the mass spectrum, widths and branching ratios in the BRpV-mSUGRA model we employed a generalized version of the SPHENO program [19]. Given the

mSUGRA parameters ($m_0, m_{1/2}, \tan\beta, \text{sign}(\mu), A_0$) SPHENO obtains a set of BRpV parameters that is compatible with the neutrino data, as well as, the masses and branching ratios, writing its output in the SLHA format [20]. We carried out the event generation using PYTHIA version 6.408 [21, 22] inputting the SLHA SPHENO output. Since the BRpV parameters consistent with neutrino data are rather small, the production takes place through the usual R-parity conserving channels contained in PYTHIA. For the same reason, the decay of all supersymmetric particles are dominated by the R-conserving modes, except for the cases that it is suppressed or forbidden, for instance, the LSP decays via R-parity violating channels.

In our analysis we looked for one detached vertex away from the primary vertex requiring it to be outside an ellipsoid around the primary vertex

$$\left(\frac{x}{\delta_{xy}}\right)^2 + \left(\frac{y}{\delta_{xy}}\right)^2 + \left(\frac{z}{\delta_z}\right)^2 = 1,$$

where the z -axis is along the beam direction and $\delta_{xy} = 20 \mu\text{m}$ and $\delta_z = 500 \mu\text{m}$. We further required that the LSP decay vertex must be inside the vertex locator sub-detector; this is a conservative requirement that can be traded by the existence of a reconstructed detached vertex in a more detailed analysis. We took into account the LHCb acceptance by considering in our study only the LSP decay products in the $1.8 < \eta < 4.9$ pseudo-rapidity range.

Within the SM, detached vertices are associated to rather long lived particles, like B 's and τ 's. Therefore, the Standard Model physics background can be eliminated by requiring that the tracks associated to the displaced vertex give rise to an invariant mass larger than 20 GeV. After imposing this cut, the neutralino displaced vertex signal is background free. Consequently, we defined that a point in the BRpV-mSUGRA parameter space is observable if 5 or more events present a detached vertex passing the above requirements for a given integrated luminosity.

Taking into account that the LHCb experiment already has a dimuon trigger, we started our analysis looking for displaced vertices associated to $\tilde{\chi}_1^0 \rightarrow \nu\mu^+\mu^-$. Despite the smallness of this branching ratio this is a very clean signal. In fact the branching ratio into this decay mode varies from a few per mil at small m_0 to a few percent at moderate and large m_0 where it origin are the two-body decays $\mu^\pm W^\mp$ and νZ .

We present in the top left panel of Figure 5 the region of the $m_0 \otimes m_{1/2}$ plane where we expect 5 or more displaced vertices for integrated luminosity of 2 fb^{-1} , $A_0 = -100 \text{ GeV}$, $\tan\beta = 10$, and $\mu > 0$. As we can see, the LHCb can discover dimuon displaced vertices for $m_{1/2}$ up to $\simeq 350$ (300) GeV for small (moderate and large) values of m_0 . These reaches correspond to neutralino masses of the order of 120–140 GeV that possess decay lengths of the order of a few millimeters. The shaded region in the top left corner of this panel of Fig. 5 is the region where the stau is the lightest supersymmetric particle. Since the stau has a very short lifetime in our BRpV-mSUGRA model, no detached vertex signal is expected in this region. Furthermore, we depicted as a hatched area the region where the production cross section for dimuon detached vertices is greater than 10 fb, therefore, leading to more than 20 background free events for an integrated luminosity of 2 fb^{-1} .

It is interesting to notice that our BRpV-mSUGRA model predicts a large number of additional purely leptonic decays of the lightest neutralino, *e.g.* $\nu\tau^+\tau^-$ or $\nu\mu^\pm e^\mp$, which possess a branching ratio similar or larger than the $\nu\mu^+\mu^-$ mode. Moreover, the relative contribution of these channels is determined by the neutrino physics [23]. Therefore, it would be important to exam them, as well, to further test the BRpV-mSUGRA model.

Since the LHCb experiment has very good vertex system we have also studied its discovery potential

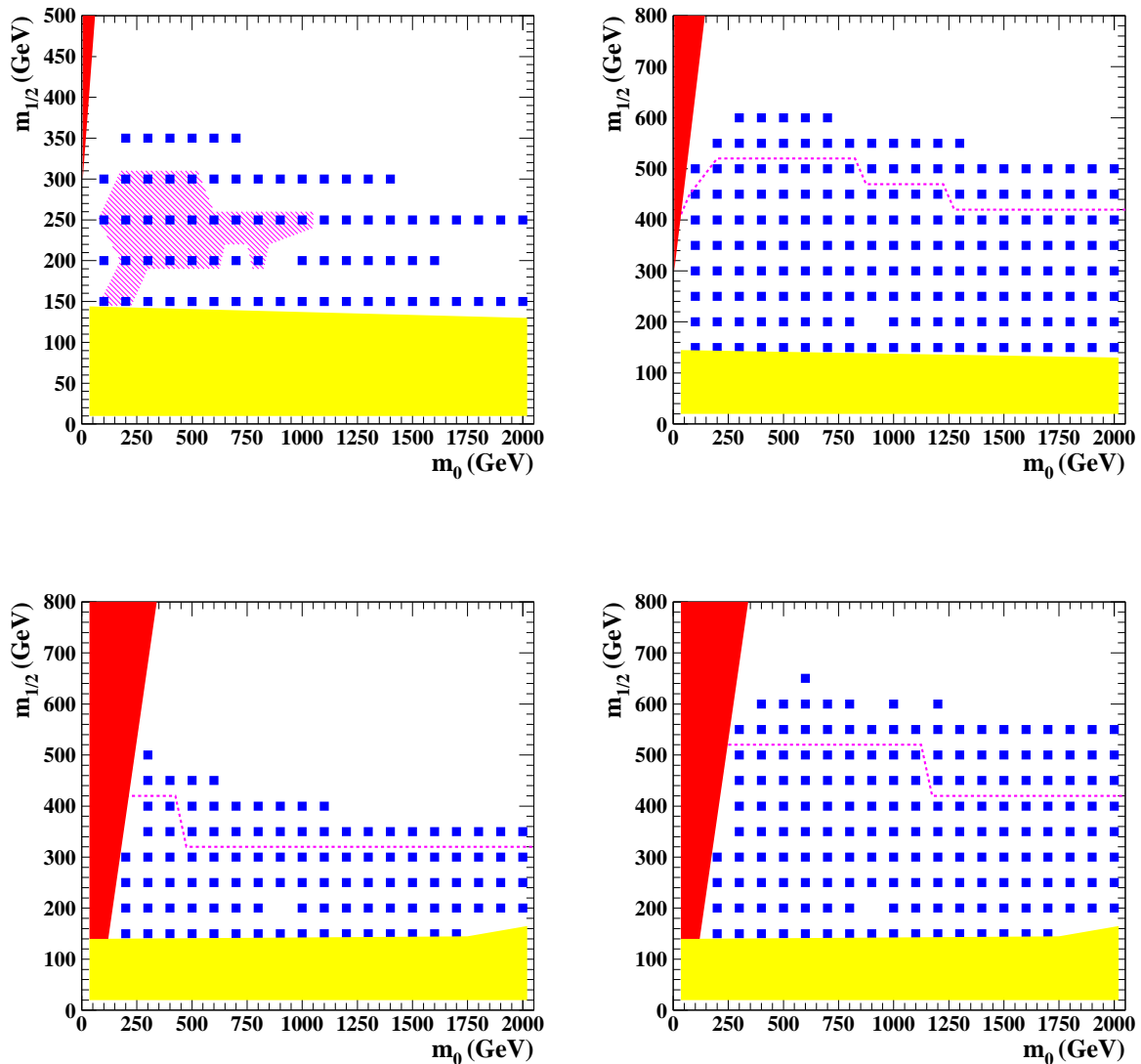


FIG. 5: The top left panel contains the LHCb discovery potential of BRpV–mSUGRA using dimuons coming from a detached vertex while the top right panel depicts the LHCb discovery potential using all visible modes. Here we assumed that $A_0 = -100$ GeV, $\tan \beta = 10$, and $\mu > 0$. The left (right) lower panel stands for the LHCb discovery potential using dimuons (all visible modes) for $\tan \beta = 40$. The blue squares stand for the points with 5 or more events for an integrated luminosity of 2 fb^{-1} . The hatched area in the left panel and the region below the dashed line in the right panel correspond to a cross section greater than 10 fb. The shaded region in the bottom is already excluded by the present available data, while the region in the top left corner of the figures indicates that the stau is the LSP.

using all LSP decays that allow vertex reconstruction, *i.e.* the decays exhibiting two or more charged particles that can be reconstructed as emanating from the same point. We present in top right panel of Figure 5 the region of the $m_0 \otimes m_{1/2}$ where 5 or more displaced vertices can be reconstructed for the same choice of parameters used in the dimuon analysis. As we can see, the inclusion of additional decay modes substantially extends the LHCb search potential to $m_{1/2} \simeq 600$ GeV at small m_0 and to $m_{1/2} \simeq 500$ GeV

at moderate and large m_0 . Therefore, the search in all visible decay mode allow us to explore neutralino masses up to 200–240 GeV and decay lengths of a few tenths of a millimeter. Notice that the LHCb reach at moderate and large m_0 is approximately independent of this parameter due to the dependence of the decay length (Figure 3) and the branching ratios (Figure 1 and 2) upon this parameter. Moreover, for most of the parameter space where the signal is observable the cross section is above 10 fb, opening the possibility of further detailed tests of the model in the event a signal is observed.

As we have seen in the previous section, the LSP decay length is rather stable against variations of the BRpV parameters provided they are in 3σ agreement with the available neutrino data. Therefore, the LHCb discovery reach does not change appreciably when the BRpV parameters are varied, except for the boundary points of the discovery region that can be shifted by a few GeV. In order to assess the impact of $\tan\beta$ changes in the search for detached vertices we present in lower panels of Figure 5 the reach of the LHCb experiment for $\tan\beta = 40$. As is well known for this value of $\tan\beta$, the region where the stau is the LSP is larger than in previous case. Therefore, the large shaded region on the left panel of this figure can not be explored via detached vertices since the stau is short lived. Furthermore, we can see that the $m_{1/2}$ reach in the dimuon channel is increased by around 30% for small and moderate m_0 ($\lesssim 1$ TeV), with the region exhibiting a production cross section in excess of 10 fb being considerably expanded. Notice that we have not indicated in this figure the small non-observable regions where the neutralino decay length is substantially reduced due to the presence of nearly degenerated states.

The lower right panel of Fig. 5 depicts the area that the detached vertex signal is visible when we consider all LSP decays that allow vertex reconstruction for $\tan\beta = 40$. In contrast with the dimuon channel, the discovery area for 2 fb^{-1} almost does not change when we vary $\tan\beta$. This stability of the LHCb reach in the visible modes could have been anticipated from the similar behavior that the neutralino branching ratios and decay length have for $\tan\beta = 10$ and 40, as seen in Figs. 3 and 4. Basically, the small changes in the branching ratios introduced by the $\tan\beta$ variation is between visible decay modes, consequently not affecting the overall signal reconstruction efficiency.

It is interesting to contrast the LHCb discovery potential with the ATLAS/CMS ones in the low luminosity initial run in order to estimate the contribution to BRvP searches that the different experiments can give. There are two main difference between the LHCb and ATLAS/CMS experiments: first of all, the ATLAS/CMS will have a luminosity 5 times the LHCb one in this period. Secondly, ATLAS/CMS vertex detectors have a larger pseudo-rapidity coverage, ranging from $-2.5 < \eta < 2.5$. Following Ref. [13], we performed the ATLAS/CMS analysis requiring the presence of two displaced vertices that satisfy the above cuts, except for the fact that we considered charged particles in the $|\eta| < 2.5$ pseudo-rapidity range.

We present in the top left panel of Fig. 6 the ATLAS/CMS reach in dimuon displaced vertices for the previous choice of parameters, $\tan\beta = 10$ and an integrated luminosity of 10 fb^{-1} . From this figure we can see that ATLAS/CMS can probe neutralino masses up to 290 GeV in dimuon displaced vertices. Comparing this figure with the top left panel of Fig. 5 we can see that ATLAS/CMS reach is a factor of 2 larger than the LHCb reach in this channel. This larger ATLAS/CMS discovery potential originates mainly from the larger planned integrated luminosity for these detectors.

The results for the search of displaced vertices at ATLAS/CMS taking into account all visible modes is presented in the top right panel of Figure 6 for $\tan\beta = 10$. As we can see form this panel, adapted from Ref. [13], ATLAS/CMS will be able to probe $m_{1/2}$ up to 800 GeV which corresponds to neutralino masses up to $\simeq 340$ GeV. Therefore, the LHCb reach in $m_{1/2}$ adding all sources of displaced vertices is around 70% the corresponding reach at ATLAS/CMS. From the rapidity coverage of the LHCb and ATLAS/CMS detectors, as well as, the prospects for the integrated luminosities, one could expected that the discovery potential of ATLAS/CMS would be considerably larger than the LHCb one. Nevertheless,

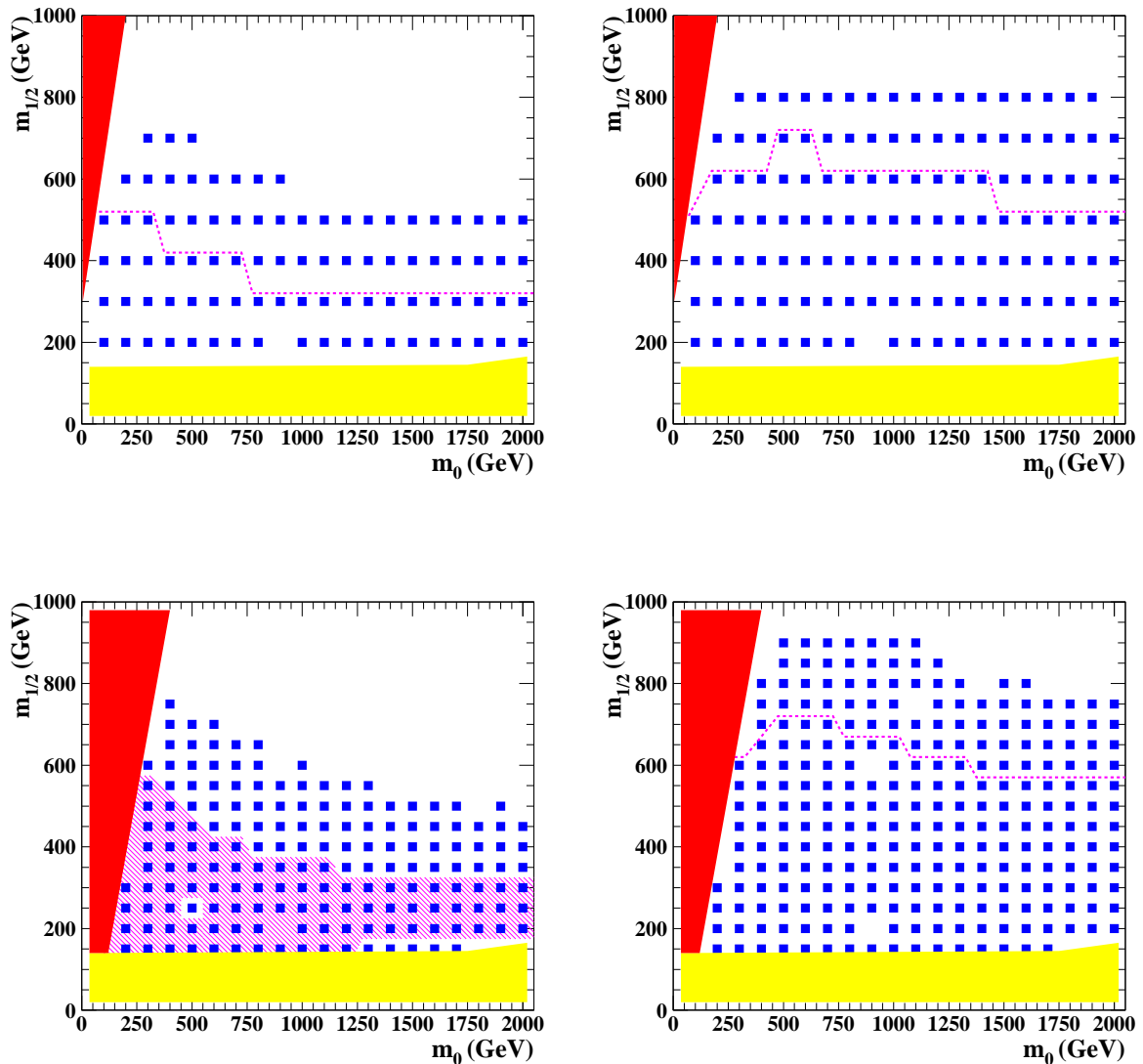


FIG. 6: Same as Figure 5 but for the ATLAS and CMS geometrical acceptance and an integrated luminosity of 10 fb^{-1} .

the reach in $m_{1/2}$ are rather similar for all experiments due to the fast decrease of the SUSY production cross section as $m_{1/2}$ increases.

The lower left (right) panel of Figure 6 contains the ATLAS/CMS discovery region in the dimuon (all visible) neutralino decay mode. First of all, it is interesting to notice that the ATLAS/CMS reach in the dimuon channel does not change significantly as we vary $\tan\beta$. In the $\tan\beta = 40$ panel one can see the effect of the drastic reduction of the neutralino decay length observed previously in Fig. 3. For instance, the cross section for the mSUGRA point $m_{1/2} = 250 \text{ GeV}$ and $m_0 = 500 \text{ GeV}$ falls down under the 10 fb region due to the reduction of the neutralino decay length. The same effect can be seen in the lower right panel for the mSUGRA point $m_{1/2} = 600 \text{ GeV}$ and $m_0 = 900 \text{ GeV}$, where the signal vanishes. Despite of this, the $m_{1/2}$ reach of these experiments is still much larger than the one expected for the LHCb. In the all visible neutralino decay mode, the ATLAS/CMS discovery reach increases as $\tan\beta$ grows. Therefore,

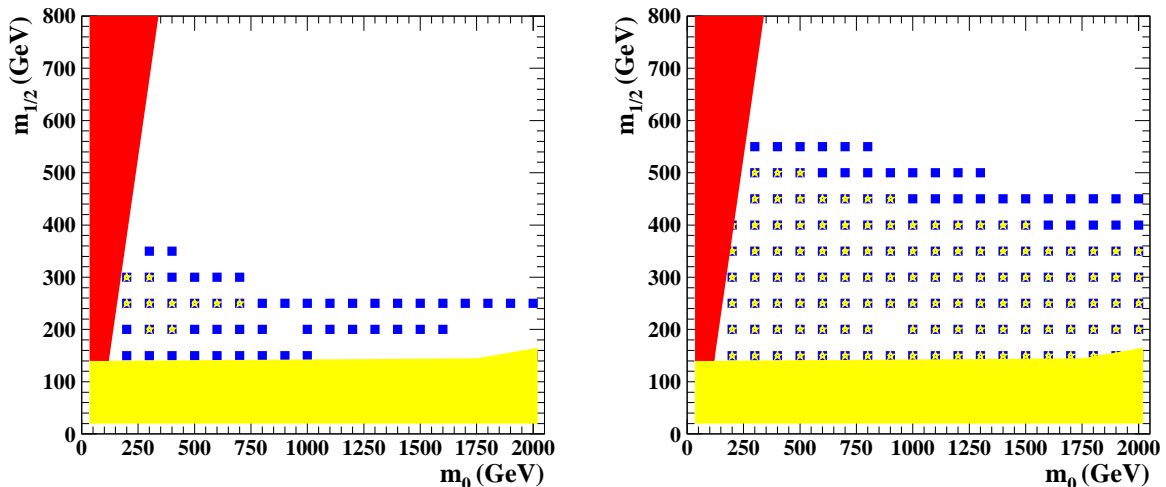


FIG. 7: Same as Figure 5 for $\tan\beta = 10$ assuming a reconstruction efficiency of 50% and no background (blue squares) or 5 background events (yellow stars).

the LHCb $m_{1/2}$ reach in this channel is $\simeq 60\%$ of the ATLAS/CMS one.

The results above should be taken with a grain of salt since our analysis did not include the trigger and reconstruction efficiencies, as well as instrumental backgrounds, which can only be estimated passing the events through a full detector simulation. In order to estimate the deterioration of the detached vertex signal we considered a reconstruction and trigger efficiency of 50% and that the number of instrumental background events is either zero or five for an integrated luminosity of 2 fb^{-1} . Figure 7 depicts the LHCb discovery potential at the 5σ level for these scenarios assuming $A_0 = -100 \text{ GeV}$, $\tan\beta = 10$, and $\mu > 0$; the background free scenario is represented by (blue) squares while the existence of 5 background events case is given by the (yellow) stars. From the left panel of Fig. 7 the inclusion of the reconstruction efficiency reduces the LHCb reach in the dimuon channel at large $m_{1/2}$. On the other hand, if there were additional background, the dimuon channel would be severely depleted. The right panel of Fig. 7 shows that the completely inclusive search is depleted at large m_0 and $m_{1/2}$ in these scenarios, however, not as much as in the dimuon topology.

Conclusions:

Our results allow us to conclude that the LHCb can search for supersymmetric models with bilinear R-parity breaking in a large fraction of the parameter space due to the additional handle provided by the existence of detached vertices in this class of models. Moreover, the discovery potential of the LHCb is rather similar (60–70%) of the ATLAS/CMS one in the low luminosity run of the LHC.

Acknowledgments

We thank J. W. F. Valle, L. de Paula, M. Gandelman and N. Gueissaz for enlightening discussions. Work supported by Conselho Nacional de Desenvolvimento Científico e Tecnológico (CNPq) and by

Fundação de Amparo à Pesquisa do Estado de São Paulo (FAPESP); by Colciencias in Colombia under contract 1115-333-18740. M. B. Magro would like to acknowledge Instituto de Física-USP for hospitality.

-
- [1] M. A. Díaz, J. C. Romão, and J. W. F. Valle, Nucl. Phys. **B524**, 23 (1998), [hep-ph/9706315].
 - [2] E. J. Chun, S. K. Kang, C. W. Kim, and U. W. Lee, Nucl. Phys. **B544**, 89 (1999); D. E. Kaplan and A. E. Nelson, JHEP **01**, 033 (2000); F. Takayama and M. Yamaguchi, Phys. Lett. **B476**, 116 (2000); T. Banks, Y. Grossman, E. Nardi, and Y. Nir, Phys. Rev. **D52**, 5319 (1995).
 - [3] M. A. Díaz *et al.*, Phys. Rev. **D68**, 013009 (2003), [hep-ph/0302021].
 - [4] M. Hirsch *et al.*, Phys. Rev. **D62**, 113008 (2000), [hep-ph/0004115], Err-ibid. **D65**:119901,2002.
 - [5] F. de Campos, M. A. Díaz, O. J. P. Éboli, M. B. Magro and P. G. Mercadante, Nucl. Phys. **B623**, 47 (2002) [arXiv:hep-ph/0110049].
 - [6] F. de Campos *et al.*, Phys. Rev. **D71**, 075001 (2005), [hep-ph/0501153].
 - [7] L. J. Hall and M. Suzuki, Nucl. Phys. **B231**, 419 (1984).
 - [8] G. G. Ross and J. W. F. Valle, Phys. Lett. **B151**, 375 (1985).
 - [9] J. R. Ellis *et al.*, Phys. Lett. **B150**, 142 (1985).
 - [10] M. Nowakowski and A. Pilaftsis (Rutherford), Nucl. Phys. **B461**, 19 (1996), [hep-ph/9508271].
 - [11] A. Masiero and J. W. F. Valle, Phys. Lett. **B251**, 273 (1990); J. C. Romão, C. A. Santos, and J. W. F. Valle, Phys. Lett. **B288**, 311 (1992); J. C. Romão, A. Ioannissyan, and J. W. F. Valle, Phys. Rev. **D55**, 427 (1997), [hep-ph/9607401].
 - [12] M. Hirsch and J. W. F. Valle, New J. Phys. **6**, 76 (2004), [hep-ph/0405015].
 - [13] F. de Campos, O. J. P. Éboli, M. B. Magro, W. Porod, D. Restrepo, M. Hirsch and J. W. F. Valle, JHEP **0805**, 048 (2008) [arXiv:0712.2156 [hep-ph]].
 - [14] M. B. Magro, F. de Campos, O. J. P. Éboli, W. Porod, D. Restrepo and J. W. F. Valle, JHEP **0309**, 071 (2003) [arXiv:hep-ph/0304232].
 - [15] D. E. Kaplan and K. Rehermann, JHEP **0710**, 056 (2007) [arXiv:0705.3426 [hep-ph]].
 - [16] A. Dedes, S. Rimmer and J. Rosiek, JHEP **0608**, 005 (2006) [arXiv:hep-ph/0603225].
 - [17] M. A. Díaz, C. Mora and A. R. Zerwekh, Eur. Phys. J. C **44**, 277 (2005) [arXiv:hep-ph/0410285].
 - [18] M. Maltoni, T. Schwetz, M. A. Tortola, and J. W. F. Valle, New J. Phys. **6**, 122 (2004), version 6 of the arXiv, hep-ph/0405172, provides results updated as of September 2007; previous works by other groups as well as the relevant experimental references are given therein.
 - [19] W. Porod, Comput. Phys. Commun. **153**, 275 (2003) [arXiv:hep-ph/0301101].
 - [20] P. Skands *et al.*, JHEP **07**, 036 (2004), [hep-ph/0311123].
 - [21] T. Sjöstrand *et al.*, Comput. Phys. Commun. **135**, 238 (2001), hep-ph/0010017.
 - [22] T. Sjöstrand, Comput. Phys. Commun. **82**, 74 (1994).
 - [23] M. Hirsch and W. Porod, Phys. Rev. D **68**, 115007 (2003) [arXiv:hep-ph/0307364].